

# Supercooling of Atoms in an Optical Resonator

Minghui Xu,<sup>1</sup> Simon B. Jäger,<sup>2</sup> S. Schütz,<sup>2</sup> J. Cooper,<sup>1</sup> Giovanna Morigi,<sup>2</sup> and M. J. Holland<sup>1</sup>

<sup>1</sup>*JILA, National Institute of Standards and Technology and Department of Physics,  
University of Colorado, Boulder, Colorado 80309-0440, USA*

<sup>2</sup>*Theoretische Physik, Universität des Saarlandes, D-66123 Saarbrücken, Germany*

(Dated: December 15, 2015)

We investigate laser cooling of an ensemble of atoms in an optical cavity. We demonstrate that when atomic dipoles are synchronized in the regime of steady-state superradiance, the motion of the atoms may be subject to a giant frictional force leading to potentially very low temperatures. The ultimate temperature limits are determined by a modified atomic linewidth, which can be orders of magnitude smaller than the cavity linewidth. The cooling rate is enhanced by the superradiant emission into the cavity mode allowing reasonable cooling rates even for dipolar transitions with ultranarrow linewidth.

PACS numbers: 37.10.Vz, 42.50.Nn, 37.30.+i, 03.65.Sq

The discovery of laser cooling [1] has enabled a new world of quantum gas physics and quantum state engineering in dilute atomic systems [2]. Laser cooling is an essential technology in many fields, including precision measurements, quantum optics, and quantum information processing [3–5]. Doppler cooling [6, 7] is perhaps the most elementary kind of laser cooling and relies on repeated cycles of electronic excitation by lasers followed by spontaneous relaxation. The temperatures that can be achieved in this way are limited by the atomic linewidth. Only specific ionic and atomic species can be Doppler cooled because they typically should possess an internal level structure that allows for closed cycling transitions.

Cavity-assisted laser cooling [8, 9] utilizes the decay of an optical resonator instead of atomic spontaneous emission as the energy dissipation mechanism. It is based on the preferential coherent scattering of laser photons into an optical cavity [10, 11], rather than absorption of free-space laser photons as in conventional Doppler cooling. Temperatures that can be achieved in cavity-assisted cooling are limited by the cavity linewidth. Since the particle properties enter only through the coherent scattering amplitude, cavity-assisted cooling promises to be applicable to any polarizable object [12–20], including molecules [17, 18] and even mesoscopic systems such as nanoparticles [19, 20].

The many-atom effects of cavity-assisted cooling were theoretically discussed by Ritsch and collaborators [21] and experimentally reported in Refs. [22, 23]. The cavity-mediated atom-atom coupling typically leads to a cooling rate that is faster for an atomic ensemble than for a single atom. Above a threshold of the pump laser, self-organization may occur and is observed as patterns in the atomic distribution that maximize the cooperative scattering. Recently, it has been shown that the long-range nature of the cavity-mediated interaction between atoms gives rise to interesting prethermalization behavior in the self-organization dynamics [24]. In spite of the intrinsic many-body nature, the underlying cooling mechanism shares much with the single-atom case, and indeed the final temperature observed in these systems is limited by the cavity linewidth.

In this paper, we demonstrate that the mechanical action of the atom-cavity coupling takes on a dramatically new character for atoms in the regime of steady-state superradiance [25–30]. Specifically, the frictional force on a single atom is significantly enhanced, and the final temperature is much lower than the temperature that can be achieved in cavity-assisted cooling [10, 11]. Furthermore, as the atom number increases, the cooling may become faster due to the increasing rate of superradiant collective emission. We show that ability to achieve much lower temperatures than for single-atom cavity-assisted cooling derives from the emergence of atom-atom dipole correlations in the many-body atomic ensemble.

Steady-state superradiant lasers were proposed in Ref. [25] as possible systems for generating millihertz linewidth light, and demonstrated in a recent experiment using a two-photon Raman transition [27]. In the regime of steady-state superradiance, the cavity decay is much faster than all other pro-

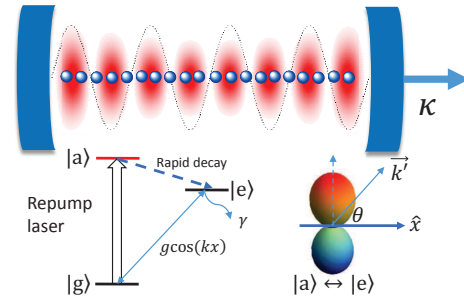


FIG. 1: (color online) Atoms with ultranarrow transition  $|g\rangle \leftrightarrow |e\rangle$  are confined to the axis of a standing-wave mode of an optical cavity. Different implementations of pumping may be considered [25, 27]. In the simplest scenario shown, a transition is driven from the ground state  $|g\rangle$  to an auxiliary state  $|a\rangle$  that rapidly decays to the excited state  $|e\rangle$ . In this way  $|a\rangle$  can be adiabatically eliminated and a two-state pseudospin description in the  $\{|g\rangle, |e\rangle\}$  subspace used, with repumping corresponding to an effective rate  $w$  from  $|g\rangle$  to  $|e\rangle$ . If the repumping laser is directed normal to the cavity axis, the absorption does not modify the momentum. Momentum recoil is induced by the on-axis component of the wavevector  $\vec{k}'$  of the dipole radiation pattern for the  $|a\rangle \leftrightarrow |e\rangle$  transition.

cesses. Therefore, the cavity mode plays the role of a dissipative collective coupling for the atoms that leads to the synchronization of atomic dipoles [29, 30]. The emergence of a macroscopic collective dipole induces an extremely narrow linewidth for the generated light [25, 30]. The optimal parameters are in the weak-coupling regime of cavity QED [31], that is opposite to the strong-coupling situation usually considered in cavity-assisted cooling [8, 9]. Superradiant lasers require weak-dipole atoms (e.g. using intercombination lines or other forbidden transitions) confined in a high-finesse optical cavity.

With this background, we now consider a specific situation of an ensemble of  $N$  point-like two-level atoms with transition frequency  $\omega_a$  and natural linewidth  $\gamma$ , interacting with a single-mode cavity with resonance frequency  $\omega_c$  and linewidth  $\kappa$ , as shown in Fig. 1. The atoms are restricted to move freely along the direction of the cavity axis ( $x$ -axis), a situation that can be realized by tightly confining the atoms in the other two directions. The atom-cavity coupling strength is given by  $g \cos(kx)$ , where  $g$  is the vacuum Rabi frequency at the field maximum and  $\cos(kx)$  describes the one-dimensional cavity mode function. The atoms are incoherently repumped at rate  $w$ , thus providing the source of photons.

The Hamiltonian describing the atom-cavity system in the rotating frame of the atomic transition frequency is given by,

$$\hat{H} = \hbar \Delta \hat{a}^\dagger \hat{a} + \sum_{j=1}^N \frac{\hat{p}_j^2}{2m} + \hbar \frac{g}{2} \sum_{j=1}^N (\hat{a}^\dagger \hat{\sigma}_j^- + \hat{\sigma}_j^+ \hat{a}) \cos(k\hat{x}_j), \quad (1)$$

where  $\Delta = \omega_c - \omega_a$ . We have introduced the bosonic annihilation and creation operators,  $\hat{a}$  and  $\hat{a}^\dagger$ , for cavity photons. The  $j$ -th atom is represented by Pauli pseudospin operators,  $\hat{\sigma}_j^z$  and  $\hat{\sigma}_j^- = (\hat{\sigma}_j^+)^{\dagger}$ , and position and momentum  $\hat{x}_j$  and  $\hat{p}_j$ , respectively.

In the presence of dissipation, the evolution of the system is described by the Born-Markov quantum master equation for the density matrix  $\hat{\rho}$  for the cavity and atoms,

$$\frac{d}{dt} \hat{\rho} = \frac{1}{i\hbar} [\hat{H}, \hat{\rho}] + \kappa \mathcal{L}[\hat{a}] \hat{\rho} + w \sum_{j=1}^N \int_{-1}^1 du N(u) \mathcal{L}[\hat{\sigma}_j^+ e^{iuk' \cdot \hat{x}_j}] \hat{\rho}, \quad (2)$$

where  $\mathcal{L}[\hat{O}] \hat{\rho} = (2\hat{O} \hat{\rho} \hat{O}^\dagger - \hat{O}^\dagger \hat{O} \hat{\rho} - \hat{\rho} \hat{O}^\dagger \hat{O})/2$  is the Lindbladian superoperator describing the incoherent processes. The term proportional to  $\kappa$  describes the cavity decay. The repumping is the term proportional to  $w$  and is modeled by spontaneous absorption with recoil [32]. The recoil is parametrized by the normalized emission pattern  $N(u)$  and wavevector  $k'$ . It will generally be a good approximation to neglect the effect of free-space spontaneous emission of the atoms out the side of the cavity, since the natural linewidth  $\gamma$  is assumed to be extremely small for atoms with an ultraweak-dipole transition.

In the parameter regime of interest, the cavity linewidth is much larger than other system frequencies, and the cavity field can be adiabatically eliminated, resulting in the phase locking of the cavity field to the collective atomic dipole [26, 29, 30]. In order to correctly encapsulate the cavity cooling mechanism, the adiabatic elimination of the cavity field has to be ex-

panded beyond the leading order. Specifically, the retardation effects between the cavity field and atomic variables should be included. As shown in the Supplemental Material [33], in the large  $\kappa$  limit [34],

$$\hat{a}(t) \approx \frac{-i \frac{g}{2} \hat{J}^-}{\kappa/2 + i\Delta} + \frac{\frac{d}{dt}(i \frac{g}{2} \hat{J}^-)}{(\kappa/2 + i\Delta)^2} - \frac{2i \sqrt{\Gamma_C}}{g} \hat{\xi}(t) + O[\kappa^{-3}], \quad (3)$$

where  $\hat{J}^- = \sum_{j=1}^N \hat{\sigma}_j^- \cos(k\hat{x}_j)$  is the collective dipole operator,  $\Gamma_C = g^2 \kappa / 4(\kappa^2/4 + \Delta^2)$  is the atomic spontaneous emission rate through the cavity, and  $\hat{\xi}(t)$  is the quantum noise originating from the vacuum field entering through the cavity output.

The dipole force on the  $j$ -th atom is given by the gradient of the potential energy, which takes the form

$$F_j = \frac{d}{dt} \hat{p}_j = -\nabla_j \hat{H} = \frac{1}{2} \hbar k g \sin(k\hat{x}_j) (\hat{\sigma}_j^+ \hat{a} + \hat{a}^\dagger \hat{\sigma}_j^-). \quad (4)$$

We maximize the single-atom dissipative force by working at the detuning  $\Delta = \kappa/2$  [33], and in that case by substituting Eq. (5) into Eq. (4) we find

$$\begin{aligned} \frac{d}{dt} \hat{p}_j \approx & -\frac{1}{2} \hbar k \Gamma_C \sin(k\hat{x}_j) \left( (1+i) \hat{\sigma}_j^+ \hat{J}^- + (1-i) \hat{J}^+ \hat{\sigma}_j^- \right) \\ & - \frac{1}{2} \eta \Gamma_C \sin(k\hat{x}_j) \sum_{l=1}^N (\hat{\sigma}_j^+ \hat{\sigma}_l^- + \hat{\sigma}_l^+ \hat{\sigma}_j^-) \frac{1}{2} [\sin(k\hat{x}_l), \hat{p}_l]_+ + \hat{N}_j. \end{aligned} \quad (5)$$

Here the anticommutator is  $[\hat{A}, \hat{B}]_+ = \hat{A}\hat{B} + \hat{B}\hat{A}$ . We have also defined  $\eta = 4\omega_r/\kappa$ , which characterizes the likelihood of a photon emission into the cavity mode in the direction of motion versus the opposite, in terms of the atomic recoil frequency  $\omega_r = \hbar k^2/2m$ . The three terms on the right hand side of Eq. (11) can be interpreted as the conservative force, the friction, and the noise-induced momentum fluctuations, respectively.

At temperatures much greater than the recoil temperature the motion is well described by a semiclassical treatment. A systematic semiclassical approximation, to make the mapping  $\langle \hat{x}_j \rangle \rightarrow x_j$  and  $\langle \hat{p}_j \rangle \rightarrow p_j$  where  $x_j$  and  $p_j$  are classical variables, is based on the symmetric ordering of operator expectation values. In order to accurately incorporate the effects of quantum noise, we match the equations of motion for the second-order moments of momenta between the quantum and semiclassical theories so that we obtain the correct momentum diffusion [33]. This procedure yields Ito stochastic equations,

$$\begin{aligned} \frac{d}{dt} p_j \approx & \hbar k \Gamma_C \sin(kx_j) \left( \text{Im}[\langle \hat{\sigma}_j^+ \hat{J}^- \rangle] - \text{Re}[\langle \hat{\sigma}_j^+ \hat{J}^- \rangle] \right) \\ & - \eta \Gamma_C \sin(kx_j) \sum_{l=1}^N \text{Re}[\langle \hat{\sigma}_j^+ \hat{\sigma}_l^- \rangle] \sin(kx_l) p_l + \xi_j^p, \end{aligned} \quad (6)$$

where  $\xi_j^p$  is the classical noise and  $\langle \xi_j^p(t) \xi_l^p(t') \rangle = D^{jl} \delta(t - t')$  with diffusion matrix

$$\begin{aligned} D^{jl} = & \hbar^2 k^2 \Gamma_C \sin(kx_j) \sin(kx_l) \text{Re}[\langle \hat{\sigma}_l^+ \hat{\sigma}_j^- \rangle] \\ & + \hbar^2 k^2 w \overline{u^2} \langle \hat{\sigma}_j^- \hat{\sigma}_l^+ \rangle \delta_{jl}, \end{aligned} \quad (7)$$

involving the geometrical average  $\overline{u^2} \equiv \int_{-1}^1 u^2 N(u) du$  and Kronecker delta  $\delta_{jl}$ . The momentum evolution is paired with the usual equation for  $x_j$

$$\frac{d}{dt}x_j = \frac{p_j}{m}. \quad (8)$$

To begin with, we first consider the case in which the effect of recoil associated with the repumping is neglected, *i.e.* we set  $k' = 0$ . This will determine the ultimate temperature limit imposed by the vacuum noise due to the cavity output. For the simple one-atom case, we can then directly find the friction ( $\alpha$ ) and diffusion ( $D$ ) coefficient from Eq. (14) and Eq. (7). The steady-state temperature  $T$  for the single atom (labeled by 1) is

$$k_B T = \frac{\langle p_1^2 \rangle}{m} = \frac{D}{2m\alpha} = \frac{\hbar\kappa}{4}, \quad (9)$$

since

$$\begin{aligned} D &= \hbar^2 k^2 \Gamma_C \sin^2(kx_1) \langle \hat{\sigma}_1^+ \hat{\sigma}_1^- \rangle, \\ \alpha &= \eta \Gamma_C \sin^2(kx_1) \langle \hat{\sigma}_1^+ \hat{\sigma}_1^- \rangle. \end{aligned} \quad (10)$$

Note that this is precisely the same temperature limit previously found in the cavity-assisted cooling case where the system is operating in the strong coupling cavity-QED region. Here the rate of the decay into the cavity mode is proportional to  $\Gamma_C \langle \hat{\sigma}_1^+ \hat{\sigma}_1^- \rangle$ , which is applicable to the weak coupling regime of cavity QED [31]. In Fig. 2(a), we show a numerical simulation of the cooling trajectory of a single atom as a function of time. As expected, the final temperature  $k_B T$  asymptotes to  $\hbar\kappa/4$  and the cooling rate is well approximated by  $R_s = \eta \Gamma_C \langle \hat{\sigma}_1^+ \hat{\sigma}_1^- \rangle$ .

The cooling in the many-atom case exhibits a distinctly different character. A feature of this model is the pseudospin-to-motion coupling of the atoms. In order to close the evolution equations of the atomic motion as described by Eq. (14) and Eq. (8), it is also necessary to solve for the dynamics of the pseudospins. For this purpose, we derive in the Supplemental Material [33] the effective quantum master equation for the pseudospins,

$$\frac{d}{dt}\hat{\rho} = \frac{1}{i\hbar}[\hat{H}_{\text{eff}}, \hat{\rho}] + \Gamma_C \mathcal{L}[\hat{J}^-]\hat{\rho} + w \sum_{j=1}^N \int_{-1}^1 du N(u) \mathcal{L}[\hat{\sigma}_j^+ e^{iuk'x_j}]\hat{\rho}, \quad (11)$$

where the effective Hamiltonian  $\hat{H}_{\text{eff}} = -\hbar\Gamma_C \hat{J}^+ \hat{J}^- / 2$  describes the coherent coupling between atoms, and the collective decay [term proportional to  $\Gamma_C$  in Eq. (11)] leads to dissipative coupling. It is the dissipative coupling that gives rise to dipole synchronization and steady-state superradiance [25–30]. The full pseudospin Hilbert space dimension scales exponentially with the number of atoms. To solve Eq. (11), we thus employ a cumulant approximation that is applicable to large atom numbers [26, 29, 30]. All nonzero observables are expanded in terms of  $\langle \hat{\sigma}_j^+ \hat{\sigma}_j^- \rangle$  and  $\langle \hat{\sigma}_j^+ \hat{\sigma}_l^- \rangle$  ( $j \neq l$ ), describing the population inversion and spin-spin correlations respectively.

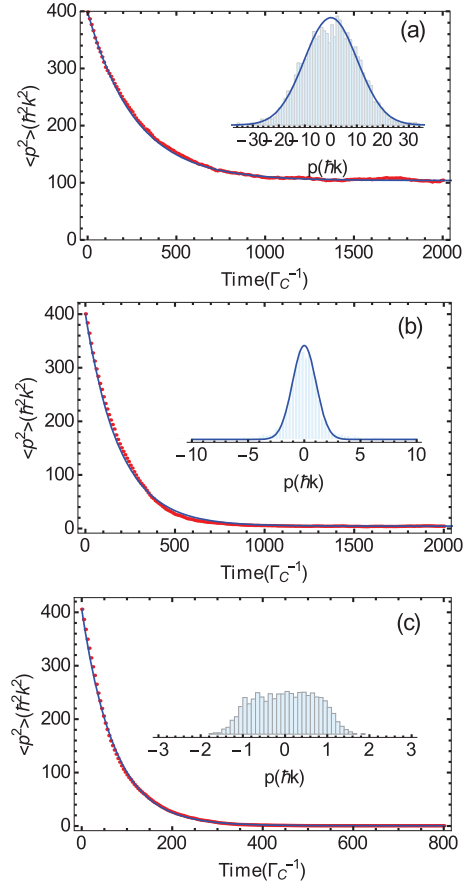


FIG. 2: (color online) Time evolution of the average momentum square (red dots) evaluated from 4000 trajectories simulated by integrating Eqs. (14) and (8) for 1 atom (a), 20 atoms (b), and 60 atoms (c). The blue solid line is a fit to an exponential decay. The parameters are  $\Delta = \kappa/2 = 100$ ,  $\Gamma_C = 0.1$ , and  $\omega_r = 0.25$ . The repumping rates are chosen such that the average atomic population inversion in all cases is the same [ $w = 0.15$  (a),  $0.28$  (b),  $1.3$  (c)]. Insets show the momentum statistics. The blue solid line is a fit to a Gaussian distribution.

Their equations of motion are derived in the Supplemental Material [33].

Simulations of the cooling dynamics for many atoms are shown in Figs. 2(b) and (c). Remarkably, we find the collective atomic effects to lead to a more rapid cooling rate, and simultaneously to generate a lower final temperature. Figure 3 shows the cooling rate (a) and the final momentum width (b) as a function of the atom number. We note that the cooling rate exhibits two kinds of behaviour, hinting towards the existence of a  $N$ -dependent threshold, see Fig. 3(a). For  $N \lesssim 20$ , the cooling rate is independent of  $N$ , while for  $N \gtrsim 20$ , it increases monotonously. Correspondingly, in this regime, the momentum width has reached a minimum which is independent of  $N$ , see Fig. 3(b). Note that when the final temperature gets closer to the recoil temperature, the momentum distribution is not Gaussian anymore, rendering the notion of temperature invalid. The semiclassical treatment predicts a uniform

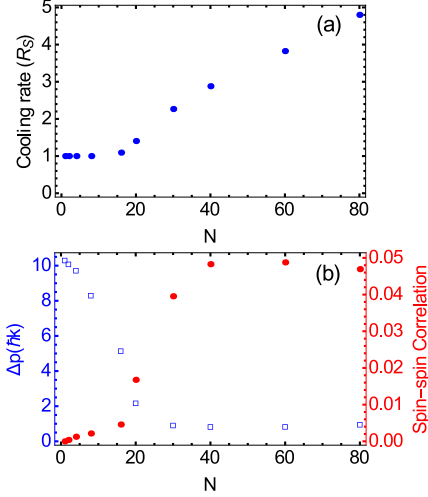


FIG. 3: (color online) (a) Cooling rate (in units of the single atom cooling rate  $R_s$ ) as a function of atom number. (b) Final momentum width ( $\Delta p = \sqrt{\langle p^2 \rangle}$ , blue squares) and spin-spin correlation (red dots) as a function of atom number. The parameters are the same as those in Fig. 2.

distribution in the momentum interval  $[-\hbar k, \hbar k]$  corresponding to the recoil limit, as shown in the inset of Fig. 2(c). These results demonstrate that for atoms in the steady-state superradiant regime, not only is the cooling more efficient due to the rapid rate of superradiant light emission, but also the final temperature is determined by the relaxation rate of the atomic dipole, and not the cavity linewidth.

The principal new feature here is that spin-spin correlations between atoms develop due to the cavity-mediated coupling. In order to measure the extent of this effect, we introduce  $\langle \hat{\sigma}^+ \hat{\sigma}^- \rangle_E$  defined as averaged spin-spin correlations,

$$\langle \hat{\sigma}^+ \hat{\sigma}^- \rangle_E = \left( \langle \hat{J}^+ \hat{J}^- \rangle - \sum_{j=1}^N \langle \hat{\sigma}_j^+ \hat{\sigma}_j^- \rangle \cos^2(kx_j) \right) / [N(N-1)]. \quad (12)$$

Fig. 3(b) shows  $\langle \hat{\sigma}^+ \hat{\sigma}^- \rangle_E$  as a function of the number of atoms. The equilibrium temperature is seen to decrease as the collective spin-spin correlation emerges. This is reminiscent of the linewidth of the superradiant laser, where the synchronization of spins leads to a significant reduction of the linewidth to the order of  $\Gamma_C$  [25, 30]. The establishment of spin-spin correlations is a competition between dephasing due to both cavity output noise and repumping, and the dissipative coupling between atoms which tends to synchronize the dipoles [30]. Since the coupling strength scales with  $N$ , a sufficient atom number is required to establish strong spin-spin correlations [30].

Further characterizing the ultimate temperature limits, Fig. 4(a) shows the final momentum width as a function of  $\Gamma_C$ . We see that as  $\Gamma_C$  is decreased, the final temperature reduces in proportion to  $\Gamma_C$  until it hits the recoil limit. This effect is consistent with a significantly increased friction coefficient pro-

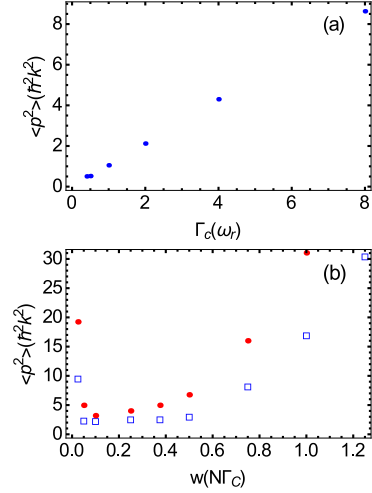


FIG. 4: (color online) (a) Final momentum width as a function of  $\Gamma_C$  for 40 atoms. The parameters are  $\Delta = \kappa/2 = 200$ ,  $w = N\Gamma_C/4$ , and  $\omega_r = 0.25$ . (b) Final momentum width as a function of repumping strength for 40 atoms without ( $k' = 0$ , blue squares) and with recoil associated with repumping ( $k' = k$ , red dots). The parameters are  $\Delta = \kappa/2 = 200$ ,  $\Gamma_C = 0.5$ , and  $\omega_r = 0.25$ .

viding a reduction of the order of the final temperature from the one to many atom case from  $\kappa$  to  $\Gamma_C$ .

So far our discussion has neglected the recoil associated with repumping. We have done that because its effect on the final temperature will depend crucially on specifics of its implementation, including factors such as the polarizations and directions of repump lasers, the atomic system, and the transitions used. However, in the specific repumping model shown in Fig. 1, the magnitude of  $k'$  controls the recoil effect of the repumping on the momentum diffusion. Fig. 4(b) shows the final momentum width as a function of repumping for  $k' = 0$  and  $k' = k$ . Again, in the region of small and large repumping, where spin-spin correlations are very small, the final temperature is high. When the recoil due to repumping is included, the final temperature becomes higher and is eventually determined by  $wu^2$ . However for weak repumping, with  $w$  not significantly larger than  $\Gamma_C$  it is still possible to achieve temperatures not much higher than that predicted when pump recoil was neglected. This is especially promising for the implementation of supercooling in realistic experimental systems. Note that  $k = k'$  is more or less a worst case scenario, since by using a dipole allowed transition for the relaxation from the auxiliary state to the excited state, one could in principle use a much reduced frequency with correspondingly small recoil.

In conclusion, we have presented a theoretical proposal for supercooling atoms in one-dimension along the axis of an optical cavity. The superradiant emission was observed to lead to an increased cooling rate and to a potentially extremely low final temperature. The ultimate temperatures were seen to be constrained by the relaxation of the atomic dipole, and could be orders of magnitude less than the limits for single atom



cooling that are constrained by the cavity linewidth. This system is an example of many-body laser cooling in which all motional degrees of freedom of a collective system are simultaneously cooled and in which macroscopic spin-spin correlations are essential and must develop for the cooling mechanism to work. It will be necessary to consider extensions to understand how cooling in all three dimensions may be achieved, and to consider realistic models for real atoms that may involve elaborate repumping schemes.

We acknowledge helpful discussions with A. M. Rey, J. Ye, and J. K. Thompson. This work has been supported by the DARPA QuASAR program, the NSF, NIST, the German Research Foundation (DACH project “Quantum crystals of matter and light”), and the German Ministry of Education and Research BMBF (Q.Com).

- 
- [1] C. E. Wieman, D. E. Pritchard, and D. J. Wineland, *Rev. Mod. Phys.* **71**, S253 (1999).
  - [2] I. Bloch, J. Dalibard, and W. Zwerger, *Rev. Mod. Phys.* **80**, 885 (2008).
  - [3] A. D. Ludlow, M. M. Boyd, J. Ye, E. Peik, and P. O. Schmidt, *Rev. Mod. Phys.* **87**, 637 (2015).
  - [4] I. A. Walmsley, *Science* **348**, 525 (2015).
  - [5] D. J. Wineland, *Rev. Mod. Phys.* **85**, 1103 (2013).
  - [6] T. W. Hänsch and A. L. Schawlow, *Opt. Commun.* **13**, 68 (1975).
  - [7] D. J. Wineland and W. M. Itano, *Phys. Rev. A* **20**, 1521 (1979).
  - [8] P. Domokos and H. Ritsch, *J. Opt. Soc. Am. B* **20**, 1098 (2003).
  - [9] H. Ritsch, P. Domokos, F. Brennecke, and T. Esslinger, *Rev. Mod. Phys.* **85**, 553 (2013).
  - [10] P. Horak, G. Hechenblaikner, K. M. Gheri, H. Stecher, and H. Ritsch, *Phys. Rev. Lett.* **79**, 4974 (1997).
  - [11] V. Vuletić and S. Chu, *Phys. Rev. Lett.* **84**, 3787 (2000).
  - [12] J. McKeever, J. R. Buck, A. D. Boozer, A. Kuzmich, H.-C. Nägerl, D. M. Stamper-Kurn, and H. J. Kimble, *Phys. Rev. Lett.* **90**, 133602 (2003).
  - [13] P. Maunz, T. Puppe, I. Schuster, N. Syassen, P. W. H. Pinkse, and G. Rempe, *Nature* **428**, 50 (2004).
  - [14] D. R. Leibbrandt, J. Labaziewicz, V. Vuletić, and I. L. Chuang, *Phys. Rev. Lett.* **103**, 103001 (2009).
  - [15] M. H. Schleier-Smith, I. D. Leroux, H. Zhang, M. A. Van Camp, and V. Vuletić, *Phys. Rev. Lett.* **107**, 143005 (2011).
  - [16] M. Wolke, J. Klinner, H. Kessler, and A. Hemmerich, *Science* **337**, 75 (2012).
  - [17] G. Morigi, P. W. H. Pinkse, M. Kowalewski, and R. deVivie-Riedle, *Phys. Rev. Lett.* **99**, 073001 (2007).
  - [18] B. L. Lev, A. Vukics, E. R. Hudson, B. C. Sawyer, P. Domokos, H. Ritsch, and J. Ye, *Phys. Rev. A* **77**, 023402 (2008).
  - [19] N. Kiesel, F. Blaser, U. Delic, D. Grass, R. Kaltenbaek, and M. Aspelmeyer, *Proc. Natl. Acad. Sci. U.S.A.* **110**, 14180 (2013).
  - [20] J. Millen, P. Z. G. Fonseca, T. Mavrogordatos, T. S. Monteiro, and P. F. Barker, *Phys. Rev. Lett.* **114**, 123602 (2015).
  - [21] P. Domokos and H. Ritsch, *Phys. Rev. Lett.* **89**, 253003 (2002).
  - [22] H. W. Chan, A. T. Black, and V. Vuletić, *Phys. Rev. Lett.* **90**, 063003 (2003).
  - [23] K. J. Arnold, M. P. Baden, and M. D. Barrett, *Phys. Rev. Lett.* **109**, 153002 (2012).
  - [24] S. Schütz and G. Morigi, *Phys. Rev. Lett.* **113**, 203002 (2014).
  - [25] D. Meiser, J. Ye, D. R. Carlson, and M. J. Holland, *Phys. Rev. Lett.* **102**, 163601 (2009).
  - [26] D. Meiser and M. J. Holland, *Phys. Rev. A* **81**, 033847 (2010); *ibid.* **81**, 063827 (2010).
  - [27] J. G. Bohnet, Z. Chen, J. M. Weiner, D. Meiser, M. J. Holland, and J. K. Thompson, *Nature* **484**, 78 (2012).
  - [28] J. G. Bohnet, Z. Chen, J. M. Weiner, K. C. Cox, and J. K. Thompson, *Phys. Rev. Lett.* **109**, 253602 (2012).
  - [29] Minghui Xu, D. A. Tieri, E. C. Fine, J. K. Thompson, and M. J. Holland, *Phys. Rev. Lett.* **113**, 154101 (2014).
  - [30] Minghui Xu and M. J. Holland, *Phys. Rev. Lett.* **114**, 103601 (2015).
  - [31] P. Meystre and M. Sargent III, *Elements of Quantum Optics* (Springer, New York, 1998).
  - [32] H. Haken, *Laser Theory* (Springer, Berlin, 1984).
  - [33] See Supplemental Material, which includes Refs. [26, 29], for the derivation of the equations for the adiabatic elimination of the cavity mode, for the external motion of atoms, and for the internal dynamics of atoms.
  - [34] This requires  $\kappa \gg \sqrt{N\bar{n}}g$ ,  $w$ , and  $k\sqrt{\langle p^2 \rangle}/m$ , where  $\bar{n}$  is the mean photon number in the cavity.

## Supplemental Material for Supercooling of Atoms in an Optical Resonator

### I. ADIABATIC ELIMINATION OF THE CAVITY MODE

The regime of steady-state superradiance is defined by a timescale separation between the single cavity mode and the atomic degrees of freedom. The typical relaxation time of the cavity mode is of the order of  $T_C \sim |\kappa + i\Delta|^{-1}$ , while the one of the atoms is given by  $T_A \sim \left(\max\{\sqrt{N\bar{n}}g, w, k\sqrt{\langle p^2 \rangle}/m\}\right)^{-1}$ , where  $\bar{n}$  is the mean photon number in the cavity. In order to eliminate the cavity field quasiadiabatically we need the relaxation time of the cavity to be much shorter than the timescale on which the atoms are evolving, namely  $T_A \gg T_C$ . To this end, we start with the quantum Langevin equation for the cavity field according to the quantum master equation [Eq. (2) in the paper],

$$\frac{d}{dt}\hat{a} = -\frac{\kappa}{2}\hat{a} - i\Delta\hat{a} - i\frac{g}{2}\hat{f}^- + \sqrt{\kappa}\hat{\xi}(t), \quad (\text{S1})$$

where  $\hat{\xi}(t)$  is the quantum white noise and  $\langle \hat{\xi}(t)\hat{\xi}^\dagger(t') \rangle = \delta(t - t')$ . The formal solution to Eq. (S1) is

$$\hat{a}(t) = e^{-(\kappa/2+i\Delta)\Delta t}\hat{a}(t_0) - i\frac{g}{2}\int_0^{\Delta t} ds e^{-(\kappa/2+i\Delta)s}\hat{f}^-(t-s) + \hat{\mathcal{F}}(t), \quad (\text{S2})$$

where  $\hat{\mathcal{F}}(t) = \sqrt{\kappa}\int_0^{\Delta t} ds e^{-(\kappa/2+i\Delta)s}\hat{\xi}(t-s)$  is the noise term and  $\Delta t = t - t_0$ . Under the approximation of coarse graining ( $T_A \gg \Delta t \gg T_C$ ), the first term on the right-hand side (RHS) of Eq. (S2) vanishes, and it can be shown that

$$\langle \hat{\mathcal{F}}(t)\hat{\mathcal{F}}^\dagger(t') \rangle \approx e^{-\kappa|t'-t|/2-i\Delta(t-t')} \approx \frac{\kappa}{\kappa^2/4 + \Delta^2}\delta(t - t'). \quad (\text{S3})$$

It would be convenient to choose  $\hat{\mathcal{F}}(t) = -i\frac{\sqrt{\Gamma_C}}{g/2}\hat{\xi}(t)$ , with

$$\Gamma_C = \frac{g^2\kappa/4}{\kappa^2/4 + \Delta^2}. \quad (\text{S4})$$

Furthermore, the integral in Eq. (S2) can be expanded in powers of  $1/(\kappa/2 + i\Delta)$ . As a result we obtain

$$\hat{a}(t) \approx \frac{-i\frac{g}{2}\hat{f}^-}{\kappa/2 + i\Delta} - \frac{\frac{d}{dt}(-i\frac{g}{2}\hat{f}^-)}{(\kappa/2 + i\Delta)^2} + \hat{\mathcal{F}}(t) + \mathcal{O}[(\kappa/2 + i\Delta)^{-3}]. \quad (\text{S5})$$

As can be seen from Eq. (S5), the retardation effects between the cavity field and atomic variables are included.

### II. EXTERNAL MOTION OF ATOMS

In this section we derive the force for the external degrees of freedom, including friction and noise. We will end up with a classical description of the particles' external degrees of freedom and derive a Langevin equation for the momenta of the particles.

The force on the  $j$ -th atom  $\hat{F}_j$  is given by

$$\hat{F}_j = \frac{d}{dt}\hat{p}_j = \hbar k \sin(k\hat{x}_j)\frac{g}{2}(\hat{\sigma}_j^+\hat{a} + \hat{a}^\dagger\hat{\sigma}_j^-) + \hat{N}_j^{\text{pump}}, \quad (\text{S6})$$

where  $\hat{N}_j^{\text{pump}}$  represents the random force due to recoil of the incoherent pumping process. Substituting Eq. (S5) into the above equation, we have

$$\begin{aligned} \frac{d}{dt}\hat{p}_j \approx & \hbar k \sin(k\hat{x}_j)\frac{\Gamma_C}{2}(-i\hat{\sigma}_j^+\hat{f}^- + i\hat{f}^+\hat{\sigma}_j^-) - \hbar k \sin(k\hat{x}_j)\frac{\Gamma_\Delta}{2}\sum_{l=1}^N \cos(kx_l)\left(\hat{\sigma}_j^+\hat{\sigma}_l^- + \hat{\sigma}_l^+\hat{\sigma}_j^- - \beta_1\hat{\sigma}_j^+\frac{d}{dt}\hat{\sigma}_l^- - \beta_1^*\frac{d}{dt}\hat{\sigma}_l^+\hat{\sigma}_j^-\right) \\ & - \sin(k\hat{x}_j)\frac{\Gamma_C}{2}\sum_{l=1}^N \frac{\eta}{2}\left[\sin(k\hat{x}_l), \hat{p}_l\right]_+ \left(\hat{\sigma}_j^+\hat{\sigma}_l^- + \hat{\sigma}_l^+\hat{\sigma}_j^- + \beta_2\hat{\sigma}_j^+\hat{\sigma}_l^- + \beta_2^*\hat{\sigma}_l^+\hat{\sigma}_j^-\right) + \hat{N}_j, \end{aligned} \quad (\text{S7})$$

where  $[\hat{A}, \hat{B}]_+ = \hat{A}\hat{B} + \hat{B}\hat{A}$  is the anticommutator and the coefficients are

$$\Gamma_\Delta = \frac{g^2\Delta/2}{\kappa^2/4 + \Delta^2}, \quad \beta_1 = \frac{\kappa}{\kappa^2/4 + \Delta^2} + i\frac{\kappa^2/4 - \Delta^2}{\Delta(\kappa^2/4 + \Delta^2)}, \quad \beta_2 = i\frac{\kappa^2/4 - \Delta^2}{\kappa\Delta}, \quad \eta = \frac{4\omega_r\Delta}{\kappa^2/4 + \Delta^2}. \quad (\text{S8})$$

Here  $\hat{N}_j = \hat{N}_j^{\text{cav}} + \hat{N}_j^{\text{pump}}$  is the sum of the noise processes originating from the cavity output  $\hat{N}_j^{\text{cav}}$  and repumping  $\hat{N}_j^{\text{pump}}$ . In the first line of equation (S7) we neglect  $\beta_1$  because in the steady state superradiance regime it holds that  $|\beta_1|\langle\hat{\sigma}_j^+\frac{d}{dt}\hat{\sigma}_l^-\rangle \sim \frac{w}{\kappa}\langle\hat{\sigma}_j^+\hat{\sigma}_l^-\rangle \ll \langle\hat{\sigma}_j^+\hat{\sigma}_l^-\rangle$ . This has also been checked numerically. Therefore we get

$$\frac{d}{dt}\hat{p}_j = \frac{d}{dt}\hat{p}_j^0 + \hat{N}_j, \quad (\text{S9})$$

where we define the force without noise as

$$\begin{aligned} \frac{d}{dt}\hat{p}_j^0 &\approx \hbar k \sin(k\hat{x}_j) \frac{\Gamma_C}{2} (-i\hat{\sigma}_j^+\hat{J}^- + i\hat{J}^+\hat{\sigma}_j^-) - \hbar k \sin(k\hat{x}_j) \frac{\Gamma_\Delta}{2} \sum_{l=1}^N \cos(kx_l) (\hat{\sigma}_j^+\hat{\sigma}_l^- + \hat{\sigma}_l^+\hat{\sigma}_j^-) \\ &\quad - \sin(k\hat{x}_j) \frac{\Gamma_C}{2} \sum_{l=1}^N \frac{\eta}{2} [\sin(k\hat{x}_l), \hat{p}_l]_+ (\hat{\sigma}_j^+\hat{\sigma}_l^- + \hat{\sigma}_l^+\hat{\sigma}_j^- + \beta_2\hat{\sigma}_j^+\hat{\sigma}_l^- + \beta_2^*\hat{\sigma}_l^+\hat{\sigma}_j^-). \end{aligned} \quad (\text{S10})$$

We work at the detuning  $\Delta = \kappa/2$  so that  $\eta$  is maximized and  $\beta_2$  vanishes. As a result we obtain

$$\frac{d}{dt}\hat{p}_j^0 \approx \hbar k \sin(k\hat{x}_j) \frac{\Gamma_C}{2} (-i\hat{\sigma}_j^+\hat{J}^- + i\hat{J}^+\hat{\sigma}_j^- - \hat{\sigma}_j^+\hat{J}^- - \hat{J}^+\hat{\sigma}_j^-) - \sin(k\hat{x}_j) \frac{\Gamma_C}{2} \sum_{l=1}^N \frac{\eta}{2} [\sin(k\hat{x}_l), \hat{p}_l]_+ (\hat{\sigma}_j^+\hat{\sigma}_l^- + \hat{\sigma}_l^+\hat{\sigma}_j^-). \quad (\text{S11})$$

The first term on the RHS of Eq. (S11) represents forces originating from the adiabatic component of the cavity field, while the second term represents the frictional force arising from retardation effects. The noise term  $\hat{N}_j$  in equation (S9) gives rise to momentum diffusion due to quantum noises associated with incoherent processes. So we derive the equations of motion for the second moments of momenta,

$$\frac{d}{dt}\langle\hat{p}_j\hat{p}_l\rangle = \left\langle\hat{p}_j^0\frac{d\hat{p}_l^0}{dt}\right\rangle + \left\langle\frac{d\hat{p}_j^0}{dt}\hat{p}_l^0\right\rangle + \Gamma_C\hbar^2k^2\langle\sin(k\hat{x}_j)\sin(k\hat{x}_l)\hat{\sigma}_j^+\hat{\sigma}_l^-\rangle + w\delta_{jl}\hbar^2k'^2\overline{u^2}\langle\hat{\sigma}_j^-\hat{\sigma}_l^+\rangle, \quad (\text{S12})$$

where  $\delta_{jl}$  is the Kronecker delta, and  $\overline{u^2}$  is the second moment of the dipole radiation pattern, *i.e.*,

$$\overline{u^2} = \int_{-1}^1 du N(u) u^2 = \frac{2}{5}, \quad (\text{S13})$$

where we have taken the dipole pattern  $N(u) = \frac{3}{2}|u|\sqrt{1-u^2}$ .

We treat the external atomic motion classically under the assumption that the momentum width of the particles  $\sqrt{\langle p^2 \rangle}$  is larger than the single photon recoil  $\hbar k$ . So we make the mapping  $\langle\hat{p}_j\rangle \rightarrow p_j$  and  $\langle\hat{x}_j\rangle \rightarrow x_j$ . As a result this leads to

$$\frac{d}{dt}p_j = \frac{d}{dt}p_j^0 + \xi_j^p, \quad (\text{S14})$$

with

$$\frac{d}{dt}p_j^0 = \hbar k \sin(kx_j) \Gamma_C (\text{Im}[\langle\hat{\sigma}_j^+\hat{J}^-\rangle] - \text{Re}[\langle\hat{\sigma}_j^+\hat{J}^-\rangle]) - \sin(kx_j) \Gamma_C \sum_{l=1}^N \eta \text{Re}[\langle\hat{\sigma}_j^+\hat{\sigma}_l^-\rangle] \sin(kx_l) p_l, \quad (\text{S15})$$

where  $\xi_j^p$  is the classical noise acting on the momentum of  $j$ -th atom and  $\langle\xi_j^p(t)\xi_l^p(t')\rangle = D^{jl}\delta(t-t')$ . The diffusion matrix  $D^{jl}$  can be computed by making quantum-classical correspondence for the second moments. According to Eq. (S14),

$$\frac{d}{dt}\langle p_j p_l \rangle = \left\langle p_j^0 \frac{dp_l^0}{dt} \right\rangle + \left\langle \frac{dp_j^0}{dt} p_l^0 \right\rangle + D^{jl}. \quad (\text{S16})$$

We use symmetric ordering of quantum operators for the quantum-classical correspondence, *i.e.*,  $\frac{1}{2}\left\langle\left[\hat{p}_j, \frac{dp_l}{dt}\right]_+\right\rangle \rightarrow \left\langle p_j \frac{dp_l}{dt} \right\rangle$ . Matching Eq. (S12) and Eq. (S16), we get

$$D^{jl} = \Gamma_C \hbar^2 k^2 \sin(kx_j) \sin(kx_l) \text{Re}[\langle\hat{\sigma}_l^+\hat{\sigma}_j^-\rangle] + w\delta_{jl}\hbar^2k'^2\overline{u^2}\langle\hat{\sigma}_j^-\hat{\sigma}_l^+\rangle. \quad (\text{S17})$$

Therefore, we could simulate the external motion of atoms with Eq. (S14) and the equation of motion for  $x_j$

$$\frac{d}{dt}x_j = \frac{p_j}{m}. \quad (\text{S18})$$

The classical noises  $\xi_j^p$  with diffusion matrix  $D^{jl}$  make sure that we have the right second order moments for momenta.

### III. INTERNAL DYNAMICS OF ATOMS

For the complete simulation of the atomic variables we also need to derive an equation for the internal degrees of freedom. In this section we will derive the equations of motions for the spins in which we drop third-order cumulants. For the internal dynamics of atoms in a superradiant laser, it is sufficient to keep the first order term in Eq. (S5),

$$\hat{a}(t) \approx -i\frac{\Gamma_C}{g}\hat{f}^- - \frac{\Gamma_\Delta}{g}\hat{f}^- + \hat{\mathcal{F}}(t). \quad (\text{S19})$$

Here, retardation effects are not included because they give rise to corrections that are of higher order and their contribution is negligible. This was also checked numerically. The adiabatic elimination of the cavity field leads to an effective quantum master equation for the atomic spins only

$$\frac{d}{dt}\rho = \frac{1}{i\hbar}[\hat{H}_{\text{eff}}, \rho] + \Gamma_C \mathcal{L}[\hat{J}^-]\rho + w \sum_{j=1}^N \int_{-1}^1 du N(u) \mathcal{L}[\hat{\sigma}_j^+ e^{i\vec{k} \cdot \vec{x}_j}]\rho, \quad (\text{S20})$$

where the Hamiltonian  $\hat{H}_{\text{eff}} = -\frac{\hbar\Gamma_\Delta}{2}\hat{J}^+\hat{J}^-$  describes the coherent coupling between each pair of atoms, and the collective decay [term  $\Gamma_C \mathcal{L}[\hat{J}^-]$  in Eq. (S20)] leads to dissipative coupling. We want to emphasize that this atomic master equation is not sufficient for the external degrees of freedom, which are treated in section II separately, and for which retardation effects are not negligible.

The spin degrees of freedom of atoms scale exponentially with the number of atoms. To solve Eq. (S20), we thus use a semiclassical approximation that is applicable to large atom numbers in the steady-state superradiance [S1, S2]. Cumulants for the expectation values of spin operators are expanded to second order. Because of the U(1) symmetry,  $\langle \hat{\sigma}_j^\pm \rangle = 0$ . Therefore, all nonzero observables are expanded in terms of  $\langle \hat{\sigma}_j^+ \hat{\sigma}_j^- \rangle$  and  $\langle \hat{\sigma}_j^+ \hat{\sigma}_l^- \rangle$  ( $j \neq l$ ). Their equations of motion can then be found from the effective master equation,

$$\begin{aligned} \frac{d}{dt}\langle \hat{\sigma}_j^+ \hat{\sigma}_j^- \rangle &= w(1 - \langle \hat{\sigma}_j^+ \hat{\sigma}_j^- \rangle) - \frac{1}{2}(\Gamma_C + i\Gamma_\Delta) \cos(k\hat{x}_j) \langle \hat{J}^+ \hat{\sigma}_j^- \rangle - \frac{1}{2}(\Gamma_C - i\Gamma_\Delta) \cos(k\hat{x}_j) \langle \hat{\sigma}_j^+ \hat{J}^- \rangle, \\ \frac{d}{dt}\langle \hat{\sigma}_j^+ \hat{\sigma}_l^- \rangle &= -w\langle \hat{\sigma}_j^+ \hat{\sigma}_l^- \rangle + \frac{1}{2}(\Gamma_C + i\Gamma_\Delta) \cos(k\hat{x}_j) \langle \hat{J}^+ \hat{\sigma}_l^- \hat{\sigma}_j^z \rangle + \frac{1}{2}(\Gamma_C - i\Gamma_\Delta) \cos(k\hat{x}_l) \langle \hat{\sigma}_l^z \hat{\sigma}_j^+ \hat{J}^- \rangle \\ &\approx -\left(w + (\Gamma_C + i\Gamma_\Delta) \cos^2(k\hat{x}_j) \langle \hat{\sigma}_j^+ \hat{\sigma}_j^- \rangle + (\Gamma_C - i\Gamma_\Delta) \cos^2(k\hat{x}_l) \langle \hat{\sigma}_l^+ \hat{\sigma}_l^- \rangle\right) \langle \hat{\sigma}_j^+ \hat{\sigma}_l^- \rangle \\ &\quad + \frac{1}{2}(\Gamma_C + i\Gamma_\Delta) \cos(k\hat{x}_j) (2\langle \hat{\sigma}_j^+ \hat{\sigma}_j^- \rangle - 1) \langle \hat{J}^+ \hat{\sigma}_l^- \rangle + \frac{1}{2}(\Gamma_C - i\Gamma_\Delta) \cos(k\hat{x}_l) (2\langle \hat{\sigma}_l^+ \hat{\sigma}_l^- \rangle - 1) \langle \hat{\sigma}_j^+ \hat{J}^- \rangle, \end{aligned} \quad (\text{S21})$$

describing the population inversion and spin-spin correlation respectively. In deriving Eq. (S21), we have dropped the third-order cumulants. In the simulations we integrate (S14), (S18) and (S21) simultaneously.

---

[S1] D. Meiser and M. J. Holland, Phys. Rev. A **81**, 033847 (2010); *ibid.* **81**, 063827 (2010).

[S2] Minghui Xu, D. A. Tieri, E. C. Fine, J. K. Thompson, and M. J. Holland, Phys. Rev. Lett. **113**, 154101 (2014).